



HAWKING RADIATION FROM NON-EVAPORATING PRIMORDIAL BLACK HOLES CANNOT ENABLE THE FORMATION OF DIRECT COLLAPSE BLACK HOLES

Jonathan Regan¹ , Marios Kalomenopoulos² , Kelly Kosmo O'Neil¹ 

[1] Department of Physics, University of Nevada, Reno

[2] Department of Physics and Astronomy, University of Nevada, Las Vegas
jonathan.regan@unlv.edu, jonathanregan12@gmail.com

November 15, 2024

ABSTRACT

The formation of supermassive black holes (SMBHs) in the early Universe is a subject of significant debate. In this study, we examine whether non-evaporating primordial black holes (PBHs) can offer a solution. We establish initial constraints on the range of PBH masses that correspond to Hawking radiation (HR) effective temperatures in the range needed to avoid the fragmentation of primordial gas into smaller, stellar-mass black holes. We also investigate the specific intensity of the HR from non-evaporating PBHs and compare it with the critical radiation needed for direct collapse black holes (DCBHs). We show that HR from non-evaporating PBHs cannot serve as the heating mechanism to facilitate the formation of the seeds for the SMBHs we observe in the high-redshift Universe unless, perhaps, the PBHs within the relevant mass range comprise a significant fraction of dark matter and are significantly clustered towards the center of the primordial halo.

Keywords Hawking Radiation · Primordial Black Holes · Direct Collapse Black Holes

Contents

1	Introduction	3
2	Hawking Radiation	4
2.1	Blackbody spectrum	4
2.1.1	Mass evolution and evaporation time	4
3	Primordial Black Holes	5
3.1	Formation	5
4	HR from PBHs as a source of DCBHs	5
4.1	Constraints from evaporation redshift	6
4.2	Constraints from X-ray feedback	6
4.3	Constraints from critical temperature	6
4.4	Constraints from critical radiation intensity	6
4.4.1	Constant distance & monochromatic PBHs	8
4.4.2	Uniform distribution & monochromatic PBHs	8
4.4.3	Isothermal distribution & monochromatic PBHs	9
4.4.4	LW background from monochromatic PBHs	9
5	Discussion	11
5.1	What happens with the production of other particles from HR?	11
5.2	Where are the ‘Greybody factors’?	12
5.3	Comparison to previous works	13
6	Conclusions	14
7	Acknowledgments	14
8	Data Availability	14
9	Appendix	14
9.1	Estimating halos sizes and masses	14
9.2	PBH evolution with redshift	15
9.3	PBH mass functions	15

1 Introduction

In the standard model of cosmology, our Universe is expanding from a hot and dense state [e.g. 1]. Astrophysical structures begin to form when initial fluctuations collapse to form the first gas clouds (also known as primordial gas clouds). These are the birthplaces of the first galaxies [e.g. 2, 3, 4, 5]. Many, if not all, of these galaxies are believed to harbor a massive black hole (BH) in their center. Observations of quasars formed in the early Universe indicate that a number of these BHs have masses of more than a billion solar masses, and were formed before the Universe was a billion years old¹. The formation of these high-mass black holes, aptly called supermassive black holes (SMBHs), is a matter of considerable debate [e.g. 11, 10].

Three of the most prevalent proposed scenarios, outlined in [11], include: 1) the collapse of massive Pop III stars and their growth due to accretion [12, 13, 14, 15], 2) runaway mergers in dense star clusters [16], and 3) the collapse of a primordial, metal-free gas cloud [17, 18, 19, 20, 21, 22, 23, 24, 25]. Alternative scenarios, among others, involve the growth of primordial black holes (PBHs) [26, 27], the increase of the mass of protostellar collapse in the presence of magnetic fields [28, 29] or gas dynamical processes [30, 31]. For a more detailed coverage of these and other scenarios, see [32, 33, 34, 35, 10, 36, 5].

Even the most common proposals are not without problems. For example, a newly-born Pop III star in the range of $\sim 100 M_{\odot}$ would need to accrete continuously at a rate close to the Eddington limit for at least a Gyr to reach masses close to $10^9 M_{\odot}$ at redshifts $z = 6 - 7$ [37, 33, 35], which poses difficulties for the first scenario. Dense star clusters would need to be able to retain their members after the mergers (i.e. to overpower the gravitational kicks that lead to the ejection of the merged object from the cluster [38, 39]), posing difficulties for the second scenario.

This paper focuses on the third scenario: the direct collapse of metal-free gas clouds, a ‘heavy seeds’ scenario. In this case, the masses of the initial BHs are on the order of $10^5 - 10^6 M_{\odot}$ [e.g. 40, 22]. Therefore, they could grow through more viable rates of accretion into the SMBHs we observe by $z \approx 6 - 7$. One of the key prerequisites of this scenario is to avoid fragmentation of the collapsing gas cloud². To avoid fragmentation, this family of models usually assumes the presence of an ‘atomic cooling halo’—a halo without significant metals or molecules that could cool efficiently and lead to fragmentation of the original cloud into smaller clumps—with an equilibrium temperature on the order of $T_{\text{crit}} \sim 10^4$ K [32, 23] (for some alternative direct-collapse scenarios see e.g. [42, 31]). To achieve such high temperatures, a number of mechanisms have been invoked [10, 43, 44, 45]. In this paper, we consider the presence of strong UV radiation in the Lyman-Werner (LW) range (11.2 – 13.6 eV) that is able to suppress the formation of molecular hydrogen H_2 [12, 46, 47, 48, 49] through radiation from PBHs.

For the heating mechanism, we investigate whether the Hawking radiation (HR) [50] emitted from early-Universe PBHs [51, 52] can create the necessary conditions for the formation of large BH seeds via the direct collapse of primordial gas clouds. In this proposed mechanism, the required energy is supplied by the HR of an evaporating PBH that is still far from “exploding”. We model this radiation as a blackbody spectrum, focusing only on primary photon emission.

The role of PBHs in the formation of the first stars and galaxies has been investigated before [53, 54, 55], but remains an important unanswered question in the scientific community. Most recently, [55] studied the heating effects of secondary HR spectra from “exploding” PBHs in primordial gas clouds. They find that in the presence of significant clustering of the PBHs in the clouds, PBHs of masses on the order of 10^{14} g can lead to a successful direct collapse of the cloud. On the other hand, [53, 54] used cosmological simulations and semi-analytical models to explore the effects of stellar-mass ($\sim 10 - 100 M_{\odot}$) PBHs in the acceleration of structure formation and gas heating by accretion feedback on the BHs. In the former case, they find that structures are similar to the ones found in Λ CDM simulations, but in latter case, they show that LW photons from accretion onto stellar-mass PBHs in the halo can indeed promote the formation of massive seeds through the direct-collapse scenario. In this work, we describe a simplified and easily-modifiable analysis framework, more in line with [55], in hopes that the scientific community can continue to build on this work to answer this open question.

For all cosmological calculations in this paper, we assume a flat Λ CDM cosmology with $H_0 = 70$ km/s/Mpc and $\Omega_m = 0.3$.

This paper is organized as follows: Section 2 reviews the main consequences of Hawking radiation. Section 3 introduces some of the relevant features of primordial black holes. Section 4 sets constraints on the primordial black holes that could act as sources of the Hawking radiation needed to produce ‘heavy seeds’, and compares these constraints with

¹Such as the quasar ULAS J1342+0928, whose SMBH has a mass of 800 million solar masses [6]. See also [7, 8, 9, 10].

²The presence of angular momentum is also an obstacle to massive BH collapse that needs to be overcome. Here, we assume that the gas clouds in question have overcome this issue by assuming they have either formed with negligible angular momentum or that they have lost their initial angular momentum due to interactions with their environment [41].

current observational limits. Finally, Section 5 provides a comprehensive discussion of the assumptions and caveats of this work and proposes extensions to this simplified model.

2 Hawking Radiation

This section provides a review of the main consequences of HR from a BH. We assume a Schwarzschild BH and consider only its primary photon emission. For a discussion on the validity of these assumptions, see Section 5.

2.1 Blackbody spectrum

The main component of HR can be modeled as a blackbody spectrum,

$$B_\nu = f_\Gamma f_{\text{ph}} \frac{2h\nu^3}{c^2} \frac{1}{\exp[h\nu/k_B T] - 1}, \quad (1)$$

where all the constants and variables have their usual meaning³ and f_{ph} refers to the percentage of HR that is in photons, with $f_{\text{ph}} = 1$ denoting the case where all of the HR is in photons. We use $f_{\text{ph}} = 0.2$ [56], unless stated otherwise. f_Γ corresponds to a constant ‘greybody’ factor of $f_\Gamma = 0.24$, as described in Section 5.2.

According to Hawking’s analysis [50], the temperature of a BH is connected to its mass via the expression

$$T_{\text{BH}} = \frac{\hbar c^3}{8\pi k_B G M_{\text{BH}}} \simeq 6.17 \times 10^{-8} \left(\frac{M_\odot}{M_{\text{BH}}} \right) \text{K}, \quad (2)$$

where M_{BH} is the mass of the black hole and G is Newton’s gravitational constant. Hence, the temperature of a BH is inversely proportional to its mass. This is a feature we will exploit in Section 4.

Eqs. (1) and (2) can then be combined to get the blackbody spectrum as a function of mass:

$$B_\nu = f_\Gamma f_{\text{ph}} \frac{2h\nu^3}{c^2} \frac{1}{\exp[16\pi^2 G M_{\text{BH}} \nu / c^3] - 1}. \quad (3)$$

2.1.1 Mass evolution and evaporation time

The energy of the emitted radiation comes from the BH, which in turn ‘loses’ its mass. As a result, the temperature of the blackbody increases, as does the peak energy of radiation, leading to increased mass loss. Equating the energy emitted to the Stefan-Boltzmann luminosity provides the evolution of the BH mass with time:

$$-\frac{dM_{\text{BH}}}{dt} c^2 = L \Rightarrow \frac{dM_{\text{BH}}}{dt} c^2 = -A\sigma T^4 = -16\pi \left(\frac{G M_{\text{BH}}}{c^2} \right)^2 \left(\frac{\hbar c^3}{8\pi G M_{\text{BH}} k_B} \right)^4, \quad (4)$$

where A is the Schwarzschild surface area and σ is the Stefan-Boltzmann constant.

Solving eq. (4), assuming $t_{\text{initial}} \rightarrow 0$, the time evolution of the BH mass since the Big Bang is:

$$M_{\text{BH}}(t) = \left[M_i^3 - \frac{3}{256} \frac{c^6 \sigma}{\pi^3 G^2} \left(\frac{\hbar}{k_B} \right)^4 t \right]^{1/3} = [M_i^3 - C \cdot t(z, H_0, \Omega_m)]^{1/3}, \quad (5)$$

with

$$C = 4.76 \times 10^{-59} M_\odot^3 / \text{Gyr}.$$

The very small value of this constant indicates that there are no significant changes in mass until the very final moments of BH evaporation.

³More specifically: ν is the frequency of emitted photons, T is the temperature of the blackbody, h is Planck’s constant, c is the speed of light, and k_B is Boltzmann’s constant.

The evaporation time t_{ev} of a BH is the amount of time required for it to completely evaporate due to the emission of HR. Setting $M_{\text{BH}}(t_{\text{ev}}) = 0$ in eq. 5, it is straightforward to find:

$$t_{\text{ev}} = \frac{15360\pi G^2 M_{\text{BH}}^3}{3\hbar c^4} = 2.1 \times 10^{67} \left(\frac{M_{\text{BH}}}{M_{\odot}} \right)^3 \text{ yr.} \quad (6)$$

As such, the maximum mass of a BH that could have evaporated due to HR within the age of the Universe (~ 13.7 Gyr) is $\sim 9 \times 10^{-20} M_{\odot}$ (or $\sim 1.8 \times 10^{14}$ g).

If one takes into account the larger variety of particles emitted as a BH evaporates (other than photons), then the evaporation time becomes shorter [57]. We comment more on this in Section 5.

Finally, the time evolution of HR temperature is given by inserting the mass evolution, eq. (5), into the HR temperature, eq. (2):

$$T = \frac{\hbar c^3}{8\pi k_B G} \frac{1}{[M_i^3 - C \cdot t(z, H_0, \Omega_m)]^{1/3}}. \quad (7)$$

For the BHs of interest in this work, the temperatures remain effectively constant over relevant timescales, as confirmed in Fig. (5a). As such, we ignore the effects of time evolution in the analysis from this point on.

3 Primordial Black Holes

This work investigates whether HR from PBHs can act as the heating mechanism of primordial gas clouds, facilitating their collapse into DCBHs. Since avoiding fragmentation requires temperatures of the order of 10^4 K, this requires BHs with masses much smaller than $1 M_{\odot}$ (see Section 4). A natural candidate for the source of HR in this scenario is primordial black holes.

3.1 Formation

PBHs are standard black holes formed in the early stages of the Universe when density fluctuations surpass a specific threshold [e.g. 51, 52, 58, 59]. PBHs are well known as possible dark matter candidates, and most importantly ones that do not require any "new physics" to explain. The birth, lifespan, and ultimate collapse of a PBH are all based on concepts of general relativity. PBHs may also contribute to a number of other phenomena including lensing, gravitational wave events, and growth of structure in the high-redshift Universe [e.g. 60].

The (maximal) mass of a PBH at formation time, assuming a period of radiation-dominated universe, is comparable to the horizon mass [61, 62]:

$$M_{\text{PBH}} \sim M_H = \frac{4}{3}\pi\rho \left(\frac{1}{H} \right)^3 \sim 10^{15} \left(\frac{t}{10^{-23}\text{s}} \right) \text{ g}, \quad (8)$$

where t is the time since the Big Bang. The reference mass of 10^{15} g corresponds to a PBH that will be evaporating today due to HR. In contrast, at $t \sim 1$ s (redshift $z \sim 10^9$ based on Λ CDM), the mass of a PBH can be on the order of $\sim 10^5 M_{\odot}$. As such, the range of possible PBH masses spans many orders of magnitudes.

PBHs have not yet been observed, but a number of constraints have been placed on them through indirect methods either via their gravitational effects or due to their radiation effects from HR [e.g. 59, 63, 64, 65]. These constraints are generally phrased in terms of the fraction of dark matter (DM) occupied by PBHs, $f_{\text{PBH}} = \rho_{\text{PBH}}/\rho_{\text{DM}}$, where $f_{\text{PBH}} = 1$ would correspond to the PBHs making up all of the DM. The filled regions of Figure 1 show some of the main observational constraints from [64]. Excluding the range of masses where f_{PBH} remains effectively unconstrained ($\sim 10^{17} - 10^{21}$ g or $10^{-17} - 10^{-12} M_{\odot}$, as well as the most massive PBHs), $f_{\text{PBH}} < 0.1$ in all of the other mass ranges. Note that the constraints are model dependent, and the numbers quoted above are optimistic limits (for some ranges, $f_{\text{PBH}} \ll 1$).

4 HR from PBHs as a source of DCBHs

The key criteria required for the formation of DCBHs in the scenario considered here include:

- The presence of an atomic cooling halo (i.e. a halo without metals or molecules that can cool efficiently and lead to fragmentation of the original cloud into smaller clumps) with an equilibrium temperature on the order of $T_{\text{crit}} \sim 10^4$ K at redshifts in the range $[z \in (10, 30)]$.
- The presence of strong UV radiation in the LW range (11.2 – 13.6 eV) that is able to suppress the formation of molecular hydrogen H_2 , and that is stronger than any simultaneous X-ray radiation.
- The presence of radiation with a strength of $J_{\text{crit}} \sim 10 - 10^5$ in conventional units of 10^{-21} erg/s/cm² /Hz/sr. For more details, see Section 4.4.

In this section, we investigate whether we can satisfy the above criteria with the presence of PBHs. In other words, in the redshift range of interest $[z \in (10, 30)]$, is it feasible for a population of PBHs to emit blackbody radiation with effective temperature T_{crit} and with enough intensity to surpass J_{crit} ?

4.1 Constraints from evaporation redshift

The scenario investigated in this work requires that the PBHs have not evaporated before $z_{\text{min}} = 10$. This sets a lower limit to the masses of PBHs of interest, i.e. $M_{\text{PBH}} > M_{\text{evap}}$. Assuming the fiducial cosmological model, $z = 10$ corresponds to an age of the universe $t_{\text{age}}(z = 10) = t_{\text{age},10} \sim 0.47$ Gyr. Equating this with evaporation time, and demanding $t_{\text{evap}} \gtrsim t_{\text{age},10}$, we get a mass constraint: $M_{\text{evap}} \gtrsim 2.8 \times 10^{-20} M_{\odot}$ (or 5.5×10^{13} g).

4.2 Constraints from X-ray feedback

X-rays can provide positive radiative feedback to star formation by enhancing production of H_2 , and hence cooling [66]. To estimate this effect, we find the PBH masses where X-rays are stronger than LW photons by calculating the ratio $B_{\text{LW}}(M_{\text{BH}})/B_{\text{X-rays}}(M_{\text{BH}}) \gtrsim 1$, taking the average energy of X-ray photons to be 1 keV and the average energy of LW photons to be 12.5 eV. This leads to a mass constraint: $M_{\text{x-ray}} \gtrsim 6.0 \times 10^{-14} M_{\odot}$ (or 1.2×10^{20} g). This constraint poses a more stringent lower limit than the evaporation constraint described above.

4.3 Constraints from critical temperature

This scenario also requires that the PBHs emit a blackbody spectrum above the threshold temperature to prevent gas fragmentation ($T_{\text{crit}} \sim 10^4$ K). This sets an upper limit to the masses of PBHs of interest, i.e. $M_{\text{PBH}} < M_{\text{crit}}$. From eq. (2), we get a mass constraint: $M_{\text{crit}} \lesssim 6.2 \times 10^{-12} M_{\odot}$ (or 1.2×10^{22} g).

The constraints reported in Sections 4.1, 4.2 and 4.3 are necessary but not sufficient conditions for PBHs to act as the appropriate heating sources for the primordial gas clouds. These constraints simply establish the range of masses that are relevant for this scenario, which is graphically depicted by the dashed lines in Figure 1. Note that these mass limits do not pose any restrictions to f_{PBH} ; they simply point to the PBH masses that are required for this mechanism to be valid. Interestingly, the T_{crit} and X-ray constraints demand masses in a region of f_{PBH} parameter space that remains predominantly open: $6.0 \times 10^{-14} M_{\odot} \lesssim M_{\text{PBH}} \lesssim 6.2 \times 10^{-12} M_{\odot}$.

4.4 Constraints from critical radiation intensity

In this section, we investigate whether it is feasible for PBHs within the mass range of interest (determined in Sections 4.1, 4.2 and 4.3) to provide the critical radiation intensity (CRI) J_{crit} needed to prevent the fragmentation of the initial cloud. CRI is given in units of erg/s/cm²/Hz/sr, and is commonly normalized with respect to $J_{21} = 10^{-21}$ erg/s/cm²/Hz/sr [47, 39, 67].

Across the literature, there are a number of different estimates for the CRI needed to keep the primordial cloud heated [e.g. 48, 68, 69, 70, 71, 49]. These estimates depend on several key features such as the relevant heating source and its spectrum, the spatial configuration of the halo, and the cosmological setting, with J_{crit} ranging from ~ 10 to 10^5 [e.g. 12, 47, 20, 45, 48, 68, 33, 72, 73].

To provide an easily-reproducible analysis framework for the scientific community, we follow [53, 54] by treating the LW radiation from the PBHs as a ‘background’ and ignoring self-shielding – the idea that a fraction of the outer layer of the gas protects the inner layer from radiation, allowing it to cool. As a result, we are able to compare the intensity of HR of PBHs with a $J_{21,\text{crit}} = 10^3$, expected for a background field of $T \gtrsim 10^4$ K [67].

A BH with Schwarzschild radius R_S emits HR with luminosity $L_{\text{LW}} = 4\pi^2 R_S^2 B_{\text{LW}}$. Its flux at distance d and solid angle $\Omega = 4\pi$ sr, assuming spherical geometry, give a specific intensity:

⁴Which can be found [here], with the official release [here].

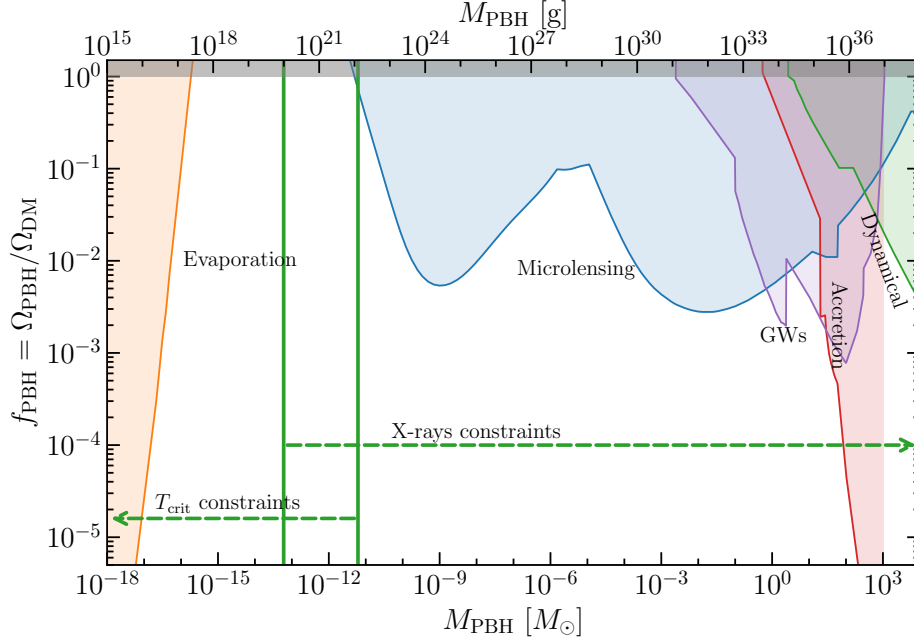


Figure 1: Constraints on the fraction of DM in PBHs from different methods (filled regions), based on [64] and plotted using PBHbounds⁴. The dashed lines show mass ranges that satisfy the respective constraints labeled above the arrows. These are physical constraints on the masses of PBHs that are needed to satisfy some of the DCBH formation criteria, as described in Sections 4.2 and 4.3. The constraints based on evaporation are not plotted here since the allowed region from that constraint spans the full plot. The y-axis values on the constraints are arbitrary and chosen for clearer visualization.

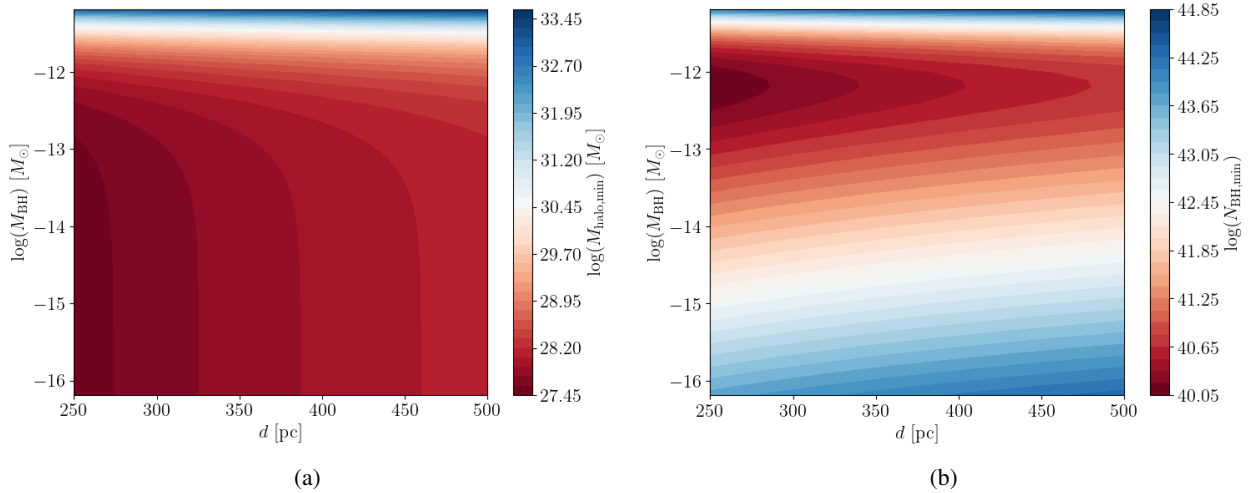


Figure 2: **(a)** Minimum estimated PBH halo mass (as a function of PBH mass and distance) that is required to produce $J_{21,LW}^{\text{tot}} \gtrsim 10^3$ for the simplest scenario considered in this work: a population of monochromatic PBHs within the mass range of interest at a distance d from a primordial gas cloud. The minimum mass of the PBH halos that satisfy this condition ($M_h \sim 10^{27.45} M_\odot$) are many orders of magnitudes larger than the most massive DM halos expected, rendering this scenario unphysical. **(b)** Same as (a), but parameterized in terms of the minimum number of PBHs that are required in order to reach $J_{21,LW}^{\text{tot}} \gtrsim 10^3$. See section 4.4.1 for more details.

$$J_{\text{LW}} = \frac{B_{\text{LW}}}{4} \left(\frac{R_{\text{S}}}{d} \right)^2. \quad (9)$$

In standard units, this becomes:

$$J_{21,\text{LW}} = 10^{21} \frac{B_{\text{LW}}}{4} \left(\frac{R_{\text{S}}}{d} \right)^2. \quad (10)$$

In the following subsections, we investigate several different PBH spatial distributions. Unless stated otherwise, we calculate PBH densities assuming the most optimistic limit of $f_{\text{PBH}} = 1$, which is allowed for the mass range found in Sections 4.1, 4.2 and 4.3. Note that we do not present results for different mass distributions because we show in Appendix 9.3 that a population of monochromatic PBHs is sufficient to test the viability of the scenario at hand.

4.4.1 Constant distance & monochromatic PBHs

The simplest case, as explored in [45, 44], is a cluster of monochromatic PBHs at a distance d from a primordial gas cloud that irradiates the cloud with LW HR photons⁵. For N_{BH} black holes of the same mass, the total intensity is $J_{21,\text{LW}}^{\text{tot}} = N_{\text{BH}} \cdot J_{21,\text{LW}}$. Demanding that $J_{21,\text{LW}}^{\text{tot}} > 10^3$, we find that $N_{\text{BH}} \geq 4 \cdot 10^{-18} (d/R_{\text{S}})^2 / B_{\text{LW}}$. Figure 2a shows an approximation of the total PBH halo mass ($M_{\text{PBH,halo}} = N_{\text{BH}} M_{\text{BH}}$) as a function of distance d for the range of allowed PBH masses. Even for the most optimistic combinations of d and M_{BH} , the total halo mass required for this scenario ($M_{\text{h}} \sim 10^{27.45} M_{\odot}$) exceeds the expected halo mass function at $z > 10$ by several orders of magnitude [e.g. 74, 75], indicating that such a configuration is not valid for the PBHs of interest here. Of course, this remains the case even if the lower limit of $J_{21,\text{LW}}$ is used. Figure 2b shows the actual number of PBHs required for a specific combination of mass and distance.

Note that here we do not consider the DCBH-formation timescale. In contrast, [45] considers a timescale of $t_{\text{coll}} \sim 10$ Myr. Both approaches are valid given the different heating mechanisms in the two situations. In [45], they consider that the LW radiation is provided by the second member of a pair of atomic cooling halos, which manages to form stars first. The latter are the source of the LW photodissociating radiation and evolve in similar timescales as the collapse. In our case, as shown in Appendix 9.2, the time evolution of PBHs is negligible for the redshift and mass ranges of interest. In other words, emission is expected to be constant for the whole period of collapse by default.

4.4.2 Uniform distribution & monochromatic PBHs

Next, we consider a population of monochromatic PBHs that are uniformly distributed inside the halo from a minimum radius r_{min} to a maximum radius r_{max} . This maximum radius is based on an estimate of the halo size, as explained in Appendix 9.1. The choice of minimum value is arbitrary, but motivated from [53], who find that stellar-mass PBHs can reach distances on the order of ~ 1 pc from the center of the DM halo. We choose $r_{\text{min}} = 1$ pc, unless stated otherwise, to be able to compare between the two scenarios.

The density of a uniform-density shell of volume $V_{\text{shell}} = 4\pi(r_{\text{max}}^3 - r_{\text{min}}^3)/3$ is given by:

$$\rho = \rho_{\text{vir}} = \rho_0 = \frac{M_{\text{tot}}}{V_{\text{shell}}} = \frac{N_{\text{BH}} M_{\text{BH}}}{V_{\text{shell}}}. \quad (11)$$

The number of PBHs within the shell is then given by:

$$N_{\text{BH}} = \frac{\rho_0}{M_{\text{BH}}} \cdot \frac{4}{3} \pi (r_{\text{max}}^3 - r_{\text{min}}^3), \quad (12)$$

or for a thin shell, the differential number of PBHs is:

$$dN_{\text{BH}} = \frac{\rho_0}{M_{\text{BH}}} \cdot 4\pi r^2 dr. \quad (13)$$

Then for the whole volume, the total LW radiation intensity at the center of the halo is:

$$J_{21,\text{LW}}^{\text{tot}} = \int_{r_{\text{min}}}^{r_{\text{max}}} dN J_{21,\text{LW}} = 10^{21} \frac{B_{\text{LW}} R_{\text{S}}^2 \rho_0}{M_{\text{BH}}} (r_{\text{max}} - r_{\text{min}}) = 10^{21} \frac{B_{\text{LW}} R_{\text{S}}^2 \rho_0 r_{\text{min}}}{M_{\text{BH}}} \left(\frac{r_{\text{max}}}{r_{\text{min}}} - 1 \right). \quad (14)$$

⁵For simplicity, we focus on photons in the middle of the energy range, i.e. we take $E_{\gamma} = 12.5$ eV. Alternatively, one can integrate $\int_{\nu_1}^{\nu_2} L_{\nu} d\nu$ and divide by $\Delta\nu$. For the distances, we adopt the range [250, 500] pc, to compare with [45]. This range avoids the halos to be tidally disrupted by their interactions, but be close enough for the LW intensity from stars to be significant.

The blue line in the top left panel of Figure 3 shows the specific intensity of LW photons at the center of a halo as a function of total halo mass. Even for the largest halo masses in this case, the radiation intensity is many orders of magnitude lower than the CRI needed to form a DCBH. Note that varying the minimum radius, redshift, and PBH mass affects the total radiation intensity slightly – as explored in the following subsection for the isothermal case – but not enough to reach the required J_{crit} . As with the case of monochromatic PBHs at a constant distance, a uniform distribution of monochromatic, non-evaporating PBHs similarly cannot enable the collapse of a DCBH.

4.4.3 Isothermal distribution & monochromatic PBHs

For a more realistic case, we investigate a monochromatic population of PBHs that follow an isothermal distribution [e.g. 44, 53]. Here, the density scales as $\rho = \rho_0 (r_{\text{max}}/r)^2$, where the density equals the virial density of the halo for $r = r_{\text{max}}$.

In this case, the total LW radiation intensity from the shell at the center of the halo is:

$$J_{21,\text{LW}}^{\text{tot}} = \int_{r_{\text{min}}}^{r_{\text{max}}} dN J_{21,\text{LW}} = 10^{21} \frac{B_{\text{LW}} R_S^2 \rho_0 r_{\text{max}}^2}{M_{\text{BH}}} \int_{r_{\text{min}}}^{r_{\text{max}}} \frac{dr}{r^2} = 10^{21} \frac{B_{\text{LW}} R_S^2 \rho_0 r_{\text{max}}}{M_{\text{BH}}} \left(\frac{r_{\text{max}}}{r_{\text{min}}} - 1 \right). \quad (15)$$

Comparing this case with eq. (14) gives:

$$J_{21}^{\text{isothermal}} = (r_{\text{max}}/r_{\text{min}}) J_{21}^{\text{uniform}}. \quad (16)$$

Since $r_{\text{max}} > r_{\text{min}}$ and thus $J_{21}^{\text{isothermal}} > J_{21}^{\text{uniform}}$, an isothermal distribution of PBHs will provide a specific intensity of LW photons that is *closer* to the required J_{crit} value than a uniform distribution of PBHs will, as demonstrated in the top left panel of Figure 3. However, even for the largest halos, the specific intensity still falls several orders of magnitude short of the required J_{crit} for this scenario.

Figure 3 also shows the effects of varying other parameters such as the minimum distance of the PBHs from the center, the formation redshift, and the PBH masses within the allowed ranges. None of these cases provide a radiation intensity that reaches the required J_{crit} value, even in the more optimistic scenario where $J_{\text{crit}} \sim 10$. We find that to reach $J_{\text{crit}} \sim 10$, in redshift $z \sim 30$ for a halo of mass $M_{\text{h}} \sim 10^{12} M_{\odot}$ – the more optimistic scenario – would require an $r_{\text{min}} \sim 3$ km. This is unphysical, if one considers that the Schwarzschild radius of a BH with $M_{\text{BH}} \sim 10^5 M_{\odot}$ (which would be the approximate mass of the seed BH at the center) would be much bigger than that.

Hence, the investigated heating mechanism provides a LW intensity many orders of magnitude smaller than critical, yielding it an ineffective way of creating the seeds of massive BHs in the early Universe.

4.4.4 LW background from monochromatic PBHs

Finally, we consider the effects of the PBHs' LW radiation acting as a cosmological background [76, 77]. To calculate the LW background, we take a similar approach to the one of the background produced by stars [78] and use:

$$J_{\text{LW},21}^{\text{bg}} = 10^{21} \frac{c}{4\pi} \int_z^{z_{\text{max}}} dz' \left| \frac{dt}{dz'} \right| \left(\frac{1+z}{1+z'} \right)^3 j_{\text{LW}}(z'), \quad (17)$$

where dt/dz' denotes the cosmic time evolution with redshift, and j_{ν} gives the proper specific intensity defined as

$$j_{\nu}(z) = L_{\nu}(z)n(z), \quad (18)$$

where L_{ν} is the luminosity of the sources and n is their number density. The maximum redshift is estimated through the ‘screening approximation’, which assumes that the LW photons can travel through the intergalactic medium until they get absorbed by a Lyman line:

$$\frac{1+z_{\text{max}}}{1+z} = \frac{\nu_{\text{abs}}}{\nu_{\text{emit}}} = f. \quad (19)$$

Based on [45], we assume $f \sim 1.04$.

Analysis of the LW background from stars in cosmological simulations provides an estimate of $J_{\text{LW},21}^{\text{bg}} \sim 3.6$ [73]. We compare this with the case of a population of monochromatic PBHs. The proper specific intensity becomes:

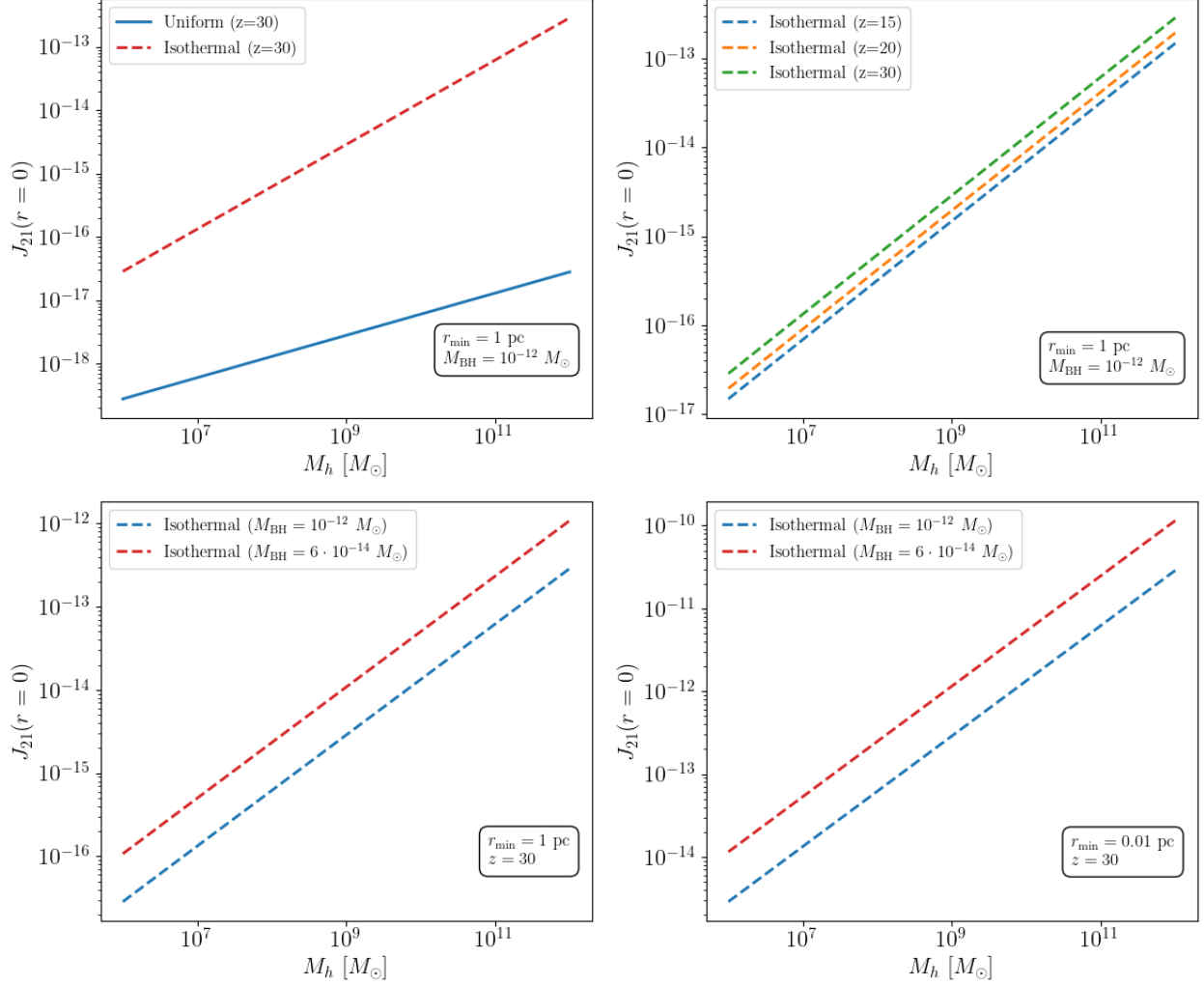


Figure 3: Specific intensity at the center of the halo for different halo masses. PBHs are distributed within the halo based on a uniform or isothermal density (Section 4.4.2 versus Section 4.4.3). The four panels of this figure investigate the effects of different density profiles (top left), of different initial redshifts of collapse (top right), of different PBH masses (bottom left), and of different minimum distances that the PBHs can reach inside the halo (bottom right). The density at r_{\max} is set to the Virial density $\rho_0 = \rho_{\text{vir}}$, as described in Appendix 9.1. The emitted specific intensity for all cases that we investigate remains orders of magnitude below the CRI required for collapse ($10 \lesssim J_{\text{crit}} \lesssim 10^5$), indicating that HR from non-evaporating PBHs is not in itself a sufficient mechanism for the formation of DCBHs in the early Universe.

$$\begin{aligned}
 j_{\text{LW}}(z) &= L_{\text{LW}}(z)n_{\text{PBH}}(z) \\
 &= \frac{L_{\text{LW}}}{M_{\text{BH}}}M_{\text{BH}}n_{\text{PBH}}(z) \\
 &= \frac{L_{\text{LW}}}{M_{\text{BH}}}f_{\text{PBH}}\rho_{\text{DM}}(z) \\
 &= \frac{L_{\text{LW}}}{M_{\text{BH}}}f_{\text{PBH}}\Omega_m(z)\rho_{\text{crit}}(z) \\
 &= \frac{4\pi^2 R_{\text{S}}^2 B_{\text{LW}}}{M_{\text{BH}}}f_{\text{PBH}}\Omega_{m,0}(1+z)^3 \frac{3H_0^2}{8\pi G},
 \end{aligned} \tag{20}$$

where we have connected the number density of PBHs to that of DM, and used the cosmological quantities defined in Appendix 9.1. Replacing $|dt/dz|$ with $1/(1+z)H(z)$ and substituting the expression for the proper specific intensity from eq. (20) into eq. (17) yields:

$$J_{\text{LW},21}^{\text{bg}} = 10^{21} \frac{c}{4\pi} \frac{4\pi^2 R_{\text{S}}^2 B_{\text{LW}}}{M_{\text{BH}}} f_{\text{PBH}} \Omega_{m,0} \frac{3H_0^2}{8\pi G} \int_z^{z_{\text{max}}} dz' \left(\frac{1+z}{1+z'} \right)^3 \frac{(1+z')^3}{(1+z')H(z')}, \tag{21}$$

which simplifies to

$$J_{\text{LW},21}^{\text{bg}} = 10^{21} \frac{cR_{\text{S}}^2 B_{\text{LW}}}{M_{\text{BH}}} f_{\text{PBH}} \Omega_{m,0} \frac{3H_0^2}{8G} (1+z)^3 \int_z^{z_{\text{max}}} dz' \frac{1}{(1+z')H(z')}. \tag{22}$$

For a quick estimate of its value, we observe that

$$\int_z^{z_{\text{max}}} dz' \frac{1}{(1+z')H(z')} \sim \frac{\Delta z}{(1+z)H(z)}, \tag{23}$$

with

$$\Delta z = z_{\text{max}} - z = (1+z_{\text{max}}) - (1+z) = (f-1)(1+z). \tag{24}$$

Finally, this leads to

$$J_{\text{LW},21}^{\text{bg}} \sim 10^{21} \frac{cR_{\text{S}}^2 B_{\text{LW}}}{M_{\text{BH}}} f_{\text{PBH}} \Omega_{m,0} \frac{3H_0^2}{8G} (1+z)^3 \frac{(f-1)}{H(z)}. \tag{25}$$

For $z = 10$ and $M_{\text{PBH}} = 10^{-12} M_{\odot}$, this results in $J_{\text{LW},21}^{\text{bg}} \sim 10^{-20}$, which is extremely small, and much smaller than the stellar contribution. Therefore, the LW background radiation from PBHs does not play any role in blocking H_2 formation.

5 Discussion

This section discusses the simplifying assumptions made in this paper, and assesses their influence on the results.

5.1 What happens with the production of other particles from HR?

In this paper, we have assumed that HR from PBHs consists only of massless particles – specifically, photons. In reality, HR can produce a variety of massless and massive particles [56, 79]. These will be important for both the radiation signature of the black hole and its evolution. We comment on these impacts in order below, but first provide a simple estimate of when these effects are important.

As mentioned in Section 2, the temperature of HR is inversely proportional to the mass of a BH. As a result, as the BH shrinks it becomes more energetic and could have enough energy to emit massive particles. Ignoring neutrinos and taking the electron as the smallest nonzero-rest-mass particle, massless particles will dominate HR when:

$$k_B T \lesssim m_e c^2 \Rightarrow M_{\text{BH}} \gtrsim \frac{\hbar c}{8\pi G m_e} \Rightarrow M_{\text{BH}} \gtrsim 6.5 \times 10^{-17} M_\odot \sim 1.3 \times 10^{17} \text{ g}. \quad (26)$$

When the BH masses are above this threshold, as is the case for the PBHs of interest in this work (see Section 4), considering only the primary spectra is a valid approximation. This regime is denoted by the region where $m_{\text{HR}} \rightarrow 0$ in Figure 4.

When the BH masses are below this threshold, massive particles start being produced⁶. These particles are not the final end products for an energetic BH since they can decay further [80, 55]. A percentage of these secondary particles would lead to the emission of additional photons – a ‘secondary spectrum’.

The effects of this extra emission are two-fold:

1. It will increase the emitted flux for a given BH. For the scenario investigated in this paper, the secondary spectra would strengthen the impact of HR by PBHs (see, for example, Figures 4 and 3 in [81] and [65] respectively). In principle, focusing only on the primary spectra makes our analysis a conservative approach. However, the impact is negligible here since the mass regime of importance to our analysis (based on the constraints in Section 4) is greater than the mass threshold where the secondary spectra become significant.
2. It will lead to an increased rate of mass loss for a BH, expediting its evaporation [57].
The mass evolution in this case is given by [57]:

$$M(t) = \left(M_i^3 - 3\alpha_{\text{eff}} \frac{\hbar c^4}{G^2} t \right)^{1/3}, \quad (27)$$

where $\alpha_{\text{eff}} = f(M)$ is a function of mass for $M_i \lesssim 10^{18}$ g, or a constant for $M_i \gtrsim 10^{18}$ g. For the ‘standard’ case we consider in this paper, $\alpha_{\text{eff}} = 1/15360\pi$. Although this would affect our determination of the evaporation time of a PBH, in the redshift and mass ranges we are considering, the PBHs are significantly far from evaporation and their evolution is effectively negligible (Figure 5a). Therefore, this will not significantly affect our results.

5.2 Where are the ‘Greybody factors’?

In the original calculation of Hawking radiation [50, 82] the number of emitted particles is

$$N_\nu = \Gamma_\nu \frac{1}{e^{h\nu/k_B T} - 1}, \quad (28)$$

where the Γ_ν term signifies the ‘greybody’ factor that modifies the spectrum from a perfect blackbody. It acts as the absorption coefficient for scattering of a scalar field off the gravitational field of a BH [82, 83]. In the short-wavelength/high-frequency limit where a photon has enough energy to surpass the effective potential due to the spacetime of the BH, this backscattering effect is small and can be ignored. To provide a quick estimate of where this limit occurs, we compare the wavelengths of the photons produced by HR with the Schwarzschild radius of the BH.

For the ‘greybody’ factors to *not* play an important role, the wavelength must be smaller than the Schwarzschild radius:

$$\lambda \lesssim R_S = \frac{2GM}{c^2} \Rightarrow M \gtrsim \frac{\hbar c^3}{2GE} \quad \text{or} \quad \nu \gtrsim \frac{c^3}{2GE}, \quad (29)$$

where $E = h\nu$ is the energy of the radiated photon, and $c = \lambda\nu$ is the speed of light. Setting $E = E_{\text{LW}} \sim 12.5$ eV for the LW energy band provides the black hole mass threshold above which the ‘greybody’ factors can be ignored:

$$M_{\text{BH}} \gtrsim 3.35 \times 10^{-11} M_\odot \sim 6.68 \times 10^{22} \text{ g}. \quad (30)$$

The regime where ‘greybody’ factors may be ignored is denoted by the region where $\Gamma_{\text{greybody}} \rightarrow 1$ in Figure 4. The mass range of the PBHs of interest in this work (see Section 4), however, lie in this regime where $\Gamma \neq 1$. As such, we

⁶This is a conservative threshold, since electrons and positrons would be ultra-relativistic at the range $m_e c^2 \ll k_B T \ll m_\mu c^2$, where m_μ is the mass of the muon. Taking this inequality into account by checking $k_B T \lesssim m_\mu c^2$, [56] estimates that the massless particles approximation will break down for masses $M_{\text{BH}} \lesssim 10^{14}$ g.

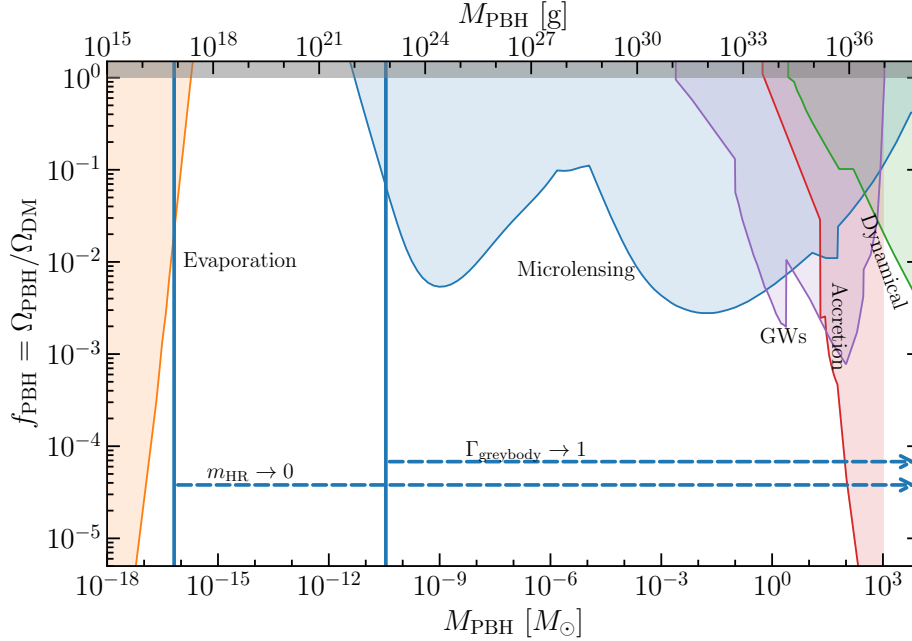


Figure 4: Similar to Figure 1, but now the dashed lines show mass ranges (specified by the arrows) where various assumptions are valid. $\Gamma_{\text{HR}} \rightarrow 0$ indicates the region where it is valid to only consider the primary HR spectra. The PBH mass range considered for this work *does* fall within this region of parameter space, and as such, we safely adhere to this assumption. $\Gamma_{\text{greybody}} \rightarrow 1$ indicates the region where it is valid to ignore greybody factors when calculating the HR spectrum. The PBH mass range considered for this work *does not* fall within this region of parameter space, and as such, we do account for a greybody factor. The y-axis values chosen for these are arbitrary and for visualization purposes only. For more details on these limits, see Sections 5.1 and 5.2.

do need to take ‘greybody’ factors into account. In principle, codes calculating Hawking radiation deal with ‘greybody’ factors in a systematic way by also monitoring all of the particles that are produced (see Section 5.1). For simplicity, we instead multiply the spectrum by a constant ‘greybody’ factor, $f_{\Gamma} = 0.24$, based on values in Section IV and Table I of [56]. This constant factor corresponds to the ratio of photon power calculated numerically with the inclusion of the necessary ‘greybody’ factors to the photon power in the high frequency/energy limit.

5.3 Comparison to previous works

As shown in Section 4.4, none of the scenarios we considered contributed enough radiation to heat the primordial gas cloud enough to avoid fragmentation. This may seem in conflict with the recent results of [55] where, under certain circumstances, PBHs were able to provide sufficient HR intensity to allow for direct collapse of the cloud. However, in reality, our work is complementary and consistent with their conclusions in the following ways:

- The main difference is that we are not considering evaporating BHs. The final ‘explosions’ of evaporating black holes produce high-energy radiation with an enhanced intensity due to the presence of significant secondary spectra. This explains the apparent disagreement with our work, which deals only with primary spectra and with masses of PBHs a few orders of magnitude bigger (and hence less energetic). Note that both mass ranges are viable; however, for our mass range, observational constraints allow $f_{\text{PBH}} = 1$, while for smaller PBHs there are severe constraints leading to $f_{\text{PBH}} < 10^{-10}$ for the global fraction of PBHs.
- In [55], they find that significant PBH clustering is necessary inside the halos – about 7 orders of magnitude bigger than the external density, i.e. $f_{\text{PBH, in}} \sim 10^7 f_{\text{PBH, out}}$ – in order for collapse to a DCBH to occur. Although the models that we investigate do not produce radiation with sufficient intensity to surpass the CRI, the fact that the isothermal distribution of PBHs gets closer to reaching the required CRI than does the uniform distribution of PBHs highlights – at least qualitatively – the importance of PBH density/clustering. Further analysis is required to determine if there are any extreme spatial distributions of PBHs within our mass range that could enable the collapse of a DCBH.

6 Conclusions

The formation of supermassive black holes at the center of distant galaxies is an open question. Direct collapse black holes offer a solution. However, they require specific conditions from a primordial gas cloud in order to be formed – namely, the gas must be heated to a sufficient level to avoid fragmentation. In this work, we considered Hawking radiation from non-evaporating primordial black holes as a potential heating source.

We used a simplified model of photon emission due to Hawking radiation from Schwarzschild black holes and calculated their specific intensity in the Lyman-Werner band, which plays a critical role in this scenario. We used physical constraints based on the evaporation timescale, X-ray emission, and temperature of primordial black holes to estimate a range of masses that is feasible for this scenario: $M_{\text{PBH}} \in (6 \cdot 10^{-14}, 6 \cdot 10^{-12}) M_{\odot}$. Interestingly, all values for the fraction of dark matter contained in primordial black holes are still allowed by observational constraints for this range of PBH masses. For PBHs within this mass range, we evaluated whether different spatial distributions of PBHs in or near a primordial gas cloud could produce the critical radiation intensity needed to prevent the fragmentation of the cloud, enabling the cloud to directly collapse into a heavy seed for the early-Universe SMBHs that have been observed.

We conclude that non-evaporating PBHs cannot provide the heating source needed to facilitate the formation of massive black hole seeds since their radiation intensity is many orders of magnitude smaller than the expected critical value $J_{\text{crit}} \sim 10^3$. Nevertheless, we exclude a range of masses of PBHs that could potentially have acted as LW ‘heating sources’. Additionally, we qualitatively confirm the importance of significant clustering of PBHs, recently proposed in the literature, when considering the effects of Hawking radiation from PBHs in preventing fragmentation of primordial gas clouds.

7 Acknowledgments

We wish to thank the authors of [55] for useful clarifications and feedback to our work. Additionally, we thank Boyan Liu for helpful comments on the PBH distributions and the analysis of LW radiation in [53], Sadegh Khochfar for bringing to our attention the X-ray constraints and providing helpful comments and references, and Charalampos Tzerefos for comments and useful references on PBHs.

8 Data Availability

We make our code public in DCBHs_HR_PBHs.

9 Appendix

9.1 Estimating halos sizes and masses

We assume a simple model for halo formation, where the mass of the collapsing DM halo is given by [4]:

$$M_{\text{vir}} = \frac{4\pi}{3} \Delta_c \rho_{\text{crit}} r_{\text{vir}}^3, \quad (31)$$

where ρ_{crit} is the critical density to make the Universe flat:

$$\rho_{\text{crit}} = \frac{3H(z)^2}{8\pi G}, \quad (32)$$

with $H(z)^2 = H_0^2[\Omega_m(1+z)^3 + 1 - \Omega_m]$. The $\Delta_c = \rho_{\text{vir}}/\rho_{\text{crit}}$ depicts the overdensity of the halo and depends on cosmology and redshift. Using the fit provided by [84] we have:

$$\Delta_c(z) = 18\pi^2 + 82y - 39y^2, \quad (33)$$

with $y = \Omega_m(z) - 1$ and $\Omega_m(z)$:

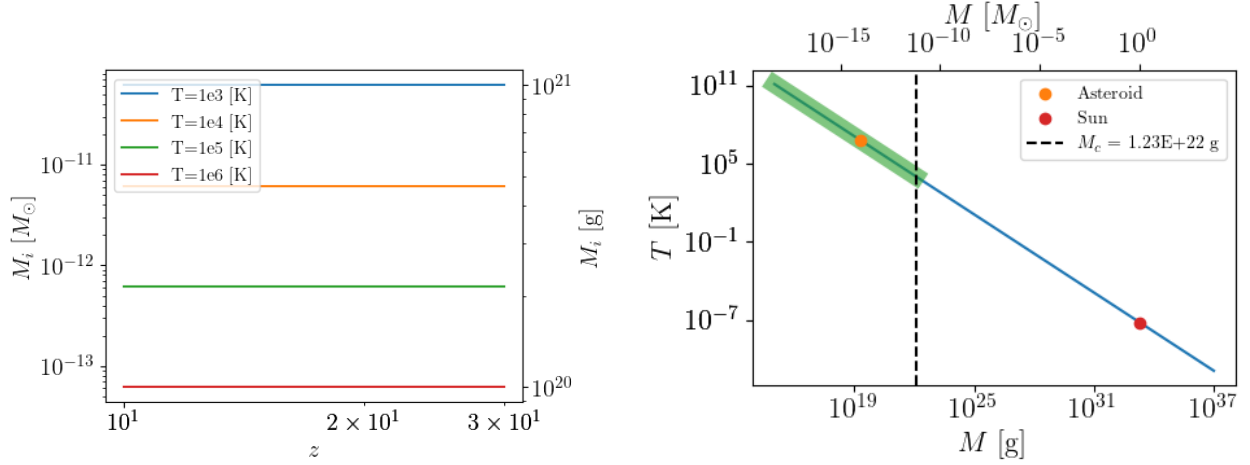
$$\Omega_m(z) = \frac{\Omega_{m,0}(1+z)^3}{\Omega_m(1+z)^3 + 1 - \Omega_m}. \quad (34)$$

Solving for the virial radius, yields:

$$r_{\text{vir}} = \left(\frac{2GM_{\text{vir}}}{\Delta_c(z)H(z)^2} \right)^{1/3}. \quad (35)$$

For a given redshift and a fixed halo mass, we use eq. (35) to get an estimate of the halo size.

Finally, the average density of the halo is given by $\rho_{\text{vir}} = \Delta_c \rho_{\text{crit}}$.



(a) Initial PBH masses for given blackbody temperatures in the redshift range of interest. In practice, the HR emitted from these BHs does not affect their mass evolution.

(b) Relationship between Hawking temperature and BH mass. Data points show the Hawking temperature of some characteristic PBH masses. The green shaded region corresponds to effective blackbody temperatures above the critical temperature required to prevent the cloud from fragmenting. The dashed line quantifies the largest possible mass allowed by this constraint.

Figure 5: (a) PBHs evolution with redshift for specific temperatures of interest, (b) Mass range with effective blackbody HR temperatures above the critical value ($T_{\text{crit}} = 10^4$).

9.2 PBH evolution with redshift

Following the discussion of Section 2, we show the evolution of BH masses due to HR in the redshift range of interest ($10 \leq z \leq 30$) for four temperatures around the critical temperature ($T_{\text{crit}} = 10^4$ K).

Figure 5a plots the initial mass of a PBH that would have a specific HR temperature as a function of redshift (found by solving eq. 7). For each temperature, the initial PBH mass needed is effectively the same for the entire range of redshifts. BH masses can only change significantly close to their evaporation time: for a PBH that would emit at around T_{crit} in the above redshift range, the evaporation time is estimated at 10^{24} Gyr, much larger than the age of the Universe. Finally, we also note that for the mass ranges considered, PBH accretion is expected to be negligible.

9.3 PBH mass functions

At the time of formation, PBHs can have a range of masses that may follow one of several proposed model-dependent mass distributions [85]. Here, we show that a population of monochromatic PBHs – which is all that we consider in the main text – is sufficient to test the viability of the scenario at hand.

To demonstrate this, we consider the factor $B_\nu R_S^2$ (the product of the specific intensity at the LW band with the squared Schwarzschild radius) since this factor plays the crucial role in determining specific intensity (see eq. 9). It is interesting to note that these two terms have an inverse behavior as a function of mass: the specific intensity gets bigger as the mass is reduced, while the Schwarzschild radius grows linearly with mass.

The mean value of this factor, $\langle B_\nu R_S^2 \rangle$, over the relevant range of masses for some mass function $P(m)$ is given by:

$$\langle B_\nu R_S^2 \rangle = \int_{M_{\text{min}}}^{M_{\text{max}}} B_\nu R_S^2 P(m) dm. \quad (36)$$

We can quantify the importance of a given mass function by comparing this mean value to the value of $B_\nu R_S^2$ calculated at each of the individual masses in the range. Figure 6 shows the $B_\nu R_S^2$ product over a range of masses compared to the mean value of this factor for an example mass function. For demonstrative purposes, the mass function considered here is a log-normal mass function⁷

⁷Where $P(m)$ is normalized to unity: $\int_0^\infty P(m) dm = 1$.

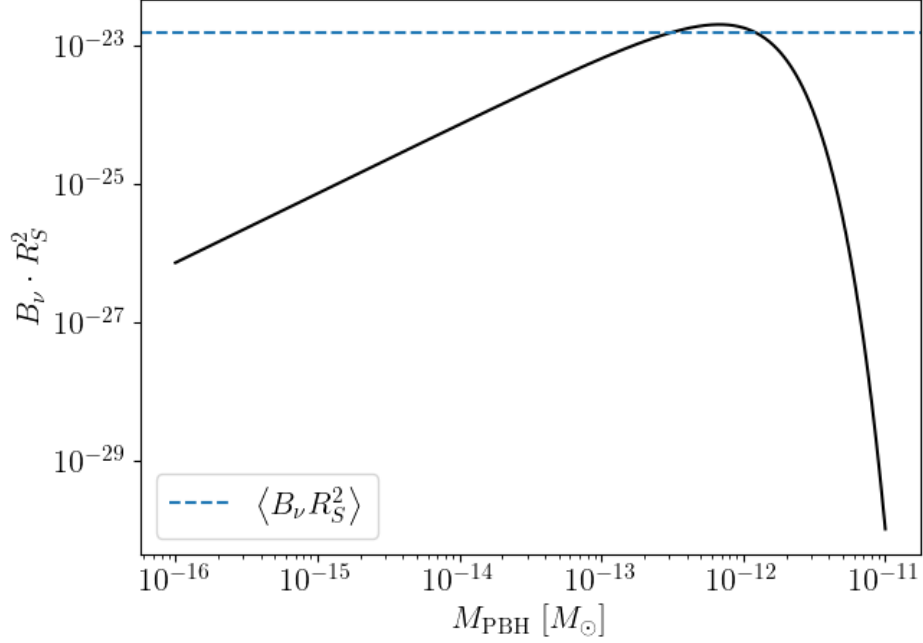


Figure 6: Change of $B_\nu R_S^2$ with PBH mass. The dashed line shows the average value from the same range of masses for a specific PBH mass function.

$$P_{LN}(m) = \frac{1}{\sigma m \sqrt{2\pi}} \exp\left(-\frac{\ln^2(m/M_c)}{2\sigma^2}\right), \quad (37)$$

where M_c denotes the median mass and σ the width of the mass distribution. Here, we chose a median mass near the peak of the $B_\nu R_S^2$ product plotted in Figure 6: $M_c = 10^{-12} M_\odot$. Note that this also explains the dip in Figure 2b. We also set $\sigma = 0.5$ so that the distribution is not very broad; however, the choice of σ does not affect the main conclusions.

Figure 6 demonstrates that a mass distribution, as expected from the properties of the mean, can outperform a number of individual masses but cannot surpass the maximum value of the $B_\nu R_S^2$ distribution. Hence, choosing a PBH mass distribution can act as an optimistic choice, but will not alter the constraints of the best monochromatic PBH scenario.

References

- [1] Particle Data Group, R L Workman, V D Burkert, V Crede, E Klempt, U Thoma, L Tiator, K Agashe, G Aielli, B C Allanach, C Amsler, M Antonelli, E C Aschenauer, D M Asner, H Baer, Sw Banerjee, R M Barnett, L Baudis, C W Bauer, J J Beatty, V I Belousov, J Beringer, A Bettini, O Biebel, K M Black, E Blucher, R Bonventre, V V Bryzgalov, O Buchmuller, M A Bychkov, R N Cahn, M Carena, A Ceccucci, A Cerri, R Sekhar Chivukula, G Cowan, K Cranmer, O Cremonesi, G D’Ambrosio, T Damour, D de Florian, A de Gouvêa, T DeGrand, P de Jong, S Demers, B A Dobrescu, M D’Onofrio, M Doser, H K Dreiner, P Eerola, U Egede, S Eidelman, A X El-Khadra, J Ellis, S C Eno, J Erler, V V Ezhela, W Fetscher, B D Fields, A Freitas, H Gallagher, Y Gershtein, T Gherghetta, M C Gonzalez-Garcia, M Goodman, C Grab, A V Gribsan, C Grojean, D E Groom, M Grünewald, A Gurtu, T Gutsche, H E Haber, Matthieu Hamel, C Hanhart, S Hashimoto, Y Hayato, A Hebecker, S Heinemeyer, J J Hernández-Rey, K Hikasa, J Hisano, A Höcker, J Holder, L Hsu, J Huston, T Hyodo, Al Ianni, M Kado, M Karliner, U F Katz, M Kenzie, V A Khoze, S R Klein, F Krauss, M Kreps, P Križan, B Krusche, Y Kwon, O Lahav, J Laiho, L P Lellouch, J Lesgourgues, A R Liddle, Z Ligeti, C-J Lin, C Lippmann, T M Liss, L Littenberg, C Lourenço, K S Lugovsky, S B Lugovsky, A Lusiani, Y Makida, F Maltoni, T Mannel, A V Manohar, W J Marciano, A Mason, J Matthews, U-G Meißner, I-A Melzer-Pellmann, M Mikhasenko, D J Miller, D Milstead, R E Mitchell, K Mönig, P Molaro, F Moortgat, M Moskovic, K Nakamura, M Narain, P Nason, S Navas, A Nelles, M Neubert, P Nevski, Y Nir, K A Olive, C Patrignani, J A Peacock, V A Petrov, E Pianori, A Pich, A Piepke, F Pietropaolo, A Pomarol, S Pordes, S Profumo, A Quadt, K Rabbertz, J Rademacker, G Raffelt, M Ramsey-Musolf, B N Ratcliff, P Richardson, A Ringwald, D J Robinson, S Roesler, S Rolli, A Romaniouk, L J Rosenberg, J L Rosner, G Rybka, M G Ryskin, R A Ryutin, Y Sakai, S Sarkar, F Sauli, O Schneider, S Schönert, K Scholberg, A J Schwartz, J Schwiening, D Scott, F Sefkow, U Seljak, V Sharma, S R Sharpe, V Shiltsev, G Signorelli, M Silari, F Simon, T Sjöstrand, P Skands, T Skwarnicki, G F Smoot, A Soffer, M S Sozzi, S Spanier, C Spiering, A Stahl, S L Stone, Y Sumino, M J Syphers, F Takahashi, M Tanabashi, J Tanaka, M Taševský, K Terao, K Terashi, J Terning, R S Thorne, M Titov, N P Tkachenko, D R Tovey, K Trabelsi, P Urquijo, G Valencia, R Van de Water, N Varelas, G Venanzoni, L Verde, I Vivarelli, P Vogel, W Vogelsang, V Vorobyev, S P Wakely, W Walkowiak, C W Walter, D Wands, D H Weinberg, E J Weinberg, N Wermes, M White, L R Wiencke, S Willocq, C G Wohl, C L Woody, W-M Yao, M Yokoyama, R Yoshida, G Zanderighi, G P Zeller, O V Zenin, R-Y Zhu, Shi-Lin Zhu, F Zimmermann, and P A Zyla. Review of Particle Physics. *Progress of Theoretical and Experimental Physics*, 2022(8):083C01, 08 2022. ISSN 2050-3911. doi: 10.1093/ptep/ptac097. URL <https://doi.org/10.1093/ptep/ptac097>.
- [2] Jarrett L. Johnson, Vecchia Claudio Dalla, and Sadegh Khochfar. The first billion years project: the impact of stellar radiation on the co-evolution of populations ii and iii. *Monthly Notices of the Royal Astronomical Society*, 428(3):1857–1872, November 2012. ISSN 0035-8711. doi: 10.1093/mnras/sts011. URL <http://dx.doi.org/10.1093/mnras/sts011>.
- [3] Hidenobu Yajima, Kentaro Nagamine, Qirong Zhu, Sadegh Khochfar, and Claudio Dalla Vecchia. Growth of first galaxies: Impacts of star formation and stellar feedback. *The Astrophysical Journal*, 846(1):30, August 2017. ISSN 1538-4357. doi: 10.3847/1538-4357/aa82b5. URL <http://dx.doi.org/10.3847/1538-4357/aa82b5>.
- [4] Andrea Cimatti, Filippo Fraternali, and Carlo Nipoti. *Introduction to Galaxy Formation and Evolution*. Cambridge University Press, 2020. ISBN 9781107134768.
- [5] Marta Volonteri, Mélanie Habouzit, and Monica Colpi. The origins of massive black holes. *Nature Reviews Physics*, 3(11):732–743, September 2021. doi: 10.1038/s42254-021-00364-9.
- [6] Eduardo Bañados, Bram P. Venemans, Chiara Mazzucchelli, Emanuele P. Farina, Fabian Walter, Feige Wang, Roberto Decarli, Daniel Stern, Xiaohui Fan, Frederick B. Davies, Joseph F. Hennawi, Robert A. Simcoe, Monica L. Turner, Hans-Walter Rix, Jinyi Yang, Daniel D. Kelson, Gwen C. Rudie, and Jan Martin Winters. An 800-million-solar-mass black hole in a significantly neutral universe at a redshift of 7.5. *Nature*, 553(7689):473–476, December 2017. ISSN 1476-4687. doi: 10.1038/nature25180. URL <http://dx.doi.org/10.1038/nature25180>.
- [7] Xue-Bing Wu, Feige Wang, Xiaohui Fan, Weimin Yi, Wenwen Zuo, Fuyan Bian, Linhua Jiang, Ian D. McGreer, Ran Wang, Jinyi Yang, Qian Yang, David Thompson, and Yuri Beletsky. An ultraluminous quasar with a twelve-billion-solar-mass black hole at redshift 6.30. *Nature*, 518(7540):512–515, February 2015. doi: 10.1038/nature14241.
- [8] Daniel J. Mortlock, Stephen J. Warren, Bram P. Venemans, Mitesh Patel, Paul C. Hewett, Richard G. McMahon, Chris Simpson, Tom Theuns, Eduardo A. González-Solares, Andy Adamson, Simon Dye, Nigel C. Hambly, Paul Hirst, Mike J. Irwin, Ernst Kuiper, Andy Lawrence, and Huub J. A. Röttgering. A luminous quasar at a redshift of $z = 7.085$. *Nature*, 474(7353):616–619, June 2011. doi: 10.1038/nature10159.
- [9] Xiaohui Fan, Michael A. Strauss, Donald P. Schneider, Robert H. Becker, Richard L. White, Zoltán Haiman, Michael Gregg, Laura Pentericci, Eva K. Grebel, Vijay K. Narayanan, Yeong-Shang Loh, Gordon T. Richards, James E. Gunn, Robert H. Lupton, Gillian R. Knapp, Željko Ivezić, W. N. Brandt, Matthew Collinge, Lei Hao,

- Daniel Harbeck, Francisco Prada, Joop Schaye, Iskra Strateva, Nadia Zakamska, Scott Anderson, Jon Brinkmann, Neta A. Bahcall, Don Q. Lamb, Sadanori Okamura, Alex Szalay, and Donald G. York. A Survey of $z > 5.7$ Quasars in the Sloan Digital Sky Survey. II. Discovery of Three Additional Quasars at $z > 6$. *The Astronomical Journal*, 125(4):1649–1659, April 2003. doi: 10.1086/368246.
- [10] Kohei Inayoshi, Eli Visbal, and Zoltán Haiman. The assembly of the first massive black holes. *Annual Review of Astronomy and Astrophysics*, 58(1):27–97, August 2020. ISSN 1545-4282. doi: 10.1146/annurev-astro-120419-014455. URL <http://dx.doi.org/10.1146/annurev-astro-120419-014455>.
- [11] Martin J. Rees. Black Hole Models for Active Galactic Nuclei. *Annual review of astronomy and astrophysics*, 22:471–506, January 1984. doi: 10.1146/annurev.aa.22.090184.002351.
- [12] Kazuyuki Omukai. Primordial Star Formation under Far-Ultraviolet Radiation. *The Astrophysical Journal*, 546(2):635–651, January 2001. doi: 10.1086/318296.
- [13] Hidenobu Yajima and Sadegh Khochfar. The role of stellar relaxation in the formation and evolution of the first massive black holes. *Monthly Notices of the Royal Astronomical Society*, 457(3):2423–2432, February 2016. ISSN 1365-2966. doi: 10.1093/mnras/stw058. URL <http://dx.doi.org/10.1093/mnras/stw058>.
- [14] Ralf Klessen. Formation of the first stars. In Muhammad Latif and Dominik Schleicher, editors, *Formation of the First Black Holes*, pages 67–97. World Scientific Publishing, 2019. doi: 10.1142/9789813227958_0004.
- [15] Muhammad A. Latif, Daniel Whalen, and Sadegh Khochfar. The birth mass function of population iii stars. *The Astrophysical Journal*, 925(1):28, January 2022. ISSN 1538-4357. doi: 10.3847/1538-4357/ac3916. URL <http://dx.doi.org/10.3847/1538-4357/ac3916>.
- [16] Harley Katz. Black hole formation in the first stellar clusters. In Muhammad Latif and Dominik Schleicher, editors, *Formation of the First Black Holes*, pages 125–143. World Scientific Publishing, 2019. doi: 10.1142/9789813227958_0007.
- [17] Mitchell C. Begelman, Marta Volonteri, and Martin J. Rees. Formation of supermassive black holes by direct collapse in pre-galactic haloes. *Monthly Notices of the Royal Astronomical Society*, 370(1):289–298, July 2006. doi: 10.1111/j.1365-2966.2006.10467.x.
- [18] Giuseppe Lodato and Priyamvada Natarajan. Supermassive black hole formation during the assembly of pre-galactic discs. *Monthly Notices of the Royal Astronomical Society*, 371(4):1813–1823, October 2006. doi: 10.1111/j.1365-2966.2006.10801.x.
- [19] Mitchell C. Begelman. Evolution of supermassive stars as a pathway to black hole formation. *Monthly Notices of the Royal Astronomical Society*, 402(1):673–681, February 2010. doi: 10.1111/j.1365-2966.2009.15916.x.
- [20] Cien Shang, Greg L. Bryan, and Z. Haiman. Supermassive black hole formation by direct collapse: keeping protogalactic gas H_2 free in dark matter haloes with virial temperatures $T_{vir} > \text{rsim } 10^4$ K. *Monthly Notices of the Royal Astronomical Society*, 402(2):1249–1262, February 2010. doi: 10.1111/j.1365-2966.2009.15960.x.
- [21] Bhaskar Agarwal, Sadegh Khochfar, Jarrett L. Johnson, Eyal Neistein, Claudio Dalla Vecchia, and Mario Livio. Ubiquitous seeding of supermassive black holes by direct collapse: Seeding of smbhs by direct collapse. *Monthly Notices of the Royal Astronomical Society*, 425(4):2854–2871, September 2012. ISSN 0035-8711. doi: 10.1111/j.1365-2966.2012.21651.x. URL <http://dx.doi.org/10.1111/j.1365-2966.2012.21651.x>.
- [22] Bhaskar Agarwal, Claudio Dalla Vecchia, Jarrett L. Johnson, Sadegh Khochfar, and Jan-Pieter Paardekooper. The first billion years project: birthplaces of direct collapse black holes. *Monthly Notices of the Royal Astronomical Society*, 443(1):648–657, July 2014. ISSN 0035-8711. doi: 10.1093/mnras/stu1112. URL <http://dx.doi.org/10.1093/mnras/stu1112>.
- [23] Bhaskar Agarwal. Primordial gas collapse in the presence of radiation: direct collapse black hole or Population III star? In Muhammad Latif and Dominik Schleicher, editors, *Formation of the First Black Holes*, pages 115–124. World Scientific Publishing, 2019. doi: 10.1142/9789813227958_0006.
- [24] Muhammad A Latif, Sadegh Khochfar, Dominik Schleicher, and Daniel J Whalen. Radiation hydrodynamical simulations of the birth of intermediate-mass black holes in the first galaxies. *Monthly Notices of the Royal Astronomical Society*, 508(2):1756–1767, September 2021. ISSN 1365-2966. doi: 10.1093/mnras/stab2708. URL <http://dx.doi.org/10.1093/mnras/stab2708>.
- [25] John Regan and Marta Volonteri. Massive Black Hole Seeds. *arXiv e-prints*, art. arXiv:2405.17975, May 2024. doi: 10.48550/arXiv.2405.17975.
- [26] Rachel Bean and João Magueijo. Could supermassive black holes be quintessential primordial black holes? *Physical Review D*, 66(6):063505, September 2002. doi: 10.1103/PhysRevD.66.063505.

- [27] Norbert Düchting. Supermassive black holes from primordial black hole seeds. *Physical Review D*, 70(6):064015, September 2004. doi: 10.1103/PhysRevD.70.064015.
- [28] Dominik R. G. Schleicher, Daniele Galli, Simon C. O. Glover, Robi Banerjee, Francesco Palla, Raffaella Schneider, and Ralf S. Klessen. The Influence of Magnetic Fields on the Thermodynamics of Primordial Star Formation. *The Astrophysical Journal*, 703(1):1096–1106, September 2009. doi: 10.1088/0004-637X/703/1/1096.
- [29] Muhammad A. Latif, Dominik R. G. Schleicher, and Sadegh Khochfar. Role of Magnetic Fields in the Formation of Direct Collapse Black Holes. *The Astrophysical Journal*, 945(2):137, March 2023. doi: 10.3847/1538-4357/acbcc2.
- [30] Muhammad A. Latif. Black hole formation via gas-dynamical processes. In Muhammad Latif and Dominik Schleicher, editors, *Formation of the First Black Holes*, pages 99–113. World Scientific Publishing, 2019. doi: 10.1142/9789813227958_0005.
- [31] M. A. Latif, D. J. Whalen, S. Khochfar, N. P. Herrington, and T. E. Woods. Turbulent cold flows gave birth to the first quasars. *Nature*, 607(7917):48–51, July 2022. doi: 10.1038/s41586-022-04813-y.
- [32] Marta Volonteri. Formation of supermassive black holes. *The Astronomy and Astrophysics Review*, 18(3):279–315, July 2010. doi: 10.1007/s00159-010-0029-x.
- [33] Muhammad A. Latif and Andrea Ferrara. Formation of Supermassive Black Hole Seeds. *Publications of the Astronomical Society of Australia*, 33:e051, October 2016. doi: 10.1017/pasa.2016.41.
- [34] Fernando Becerra. *Formation of Supermassive Black Hole Seeds in the First Galaxies*. PhD thesis, Harvard University, 2018.
- [35] Aaron Smith and Volker Bromm. Supermassive black holes in the early universe. *Contemporary Physics*, 60(2): 111–126, April 2019. doi: 10.1080/00107514.2019.1615715.
- [36] L. Haemmerlé, L. Mayer, R. S. Klessen, T. Hosokawa, P. Madau, and V. Bromm. Formation of the First Stars and Black Holes. *Space Science Reviews*, 216(4):48, April 2020. doi: 10.1007/s11214-020-00673-y.
- [37] Miloš Milosavljević, Volker Bromm, Sean M. Couch, and S. Peng Oh. Accretion onto “Seed” Black Holes in the First Galaxies. *The Astrophysical Journal*, 698(1):766–780, June 2009. doi: 10.1088/0004-637X/698/1/766.
- [38] David Merritt, Miloš Milosavljević, Marc Favata, Scott A. Hughes, and Daniel E. Holz. Consequences of Gravitational Radiation Recoil. *The Astrophysical Journal*, 607(1):L9–L12, May 2004. doi: 10.1086/421551.
- [39] Abraham Loeb and Steven R. Furlanetto. *The First Galaxies in the Universe*. Princeton University Press, 2013.
- [40] T. E. Woods, Alexander Heger, Daniel J. Whalen, Lionel Haemmerlé, and Ralf S. Klessen. On the Maximum Mass of Accreting Primordial Supermassive Stars. *The Astrophysical Journal Letters*, 842(1):L6, June 2017. doi: 10.3847/2041-8213/aa7412.
- [41] Savvas M. Koushiappas, James S. Bullock, and Avishai Dekel. Massive black hole seeds from low angular momentum material. *Monthly Notices of the Royal Astronomical Society*, 354(1):292–304, October 2004. doi: 10.1111/j.1365-2966.2004.08190.x.
- [42] Lucio Mayer and Silvia Bonoli. The route to massive black hole formation via merger-driven direct collapse: a review. *Reports on Progress in Physics*, 82(1):016901, January 2019. doi: 10.1088/1361-6633/aad6a5.
- [43] John A. Regan, John H. Wise, Brian W. O’Shea, and Michael L. Norman. The emergence of the first star-free atomic cooling haloes in the Universe. *Monthly Notices of the Royal Astronomical Society*, 492(2):3021–3031, February 2020. doi: 10.1093/mnras/staa035.
- [44] John H. Wise, John A. Regan, Brian W. O’Shea, Michael L. Norman, Turlough P. Downes, and Hao Xu. Formation of massive black holes in rapidly growing pre-galactic gas clouds. *Nature*, 566(7742):85–88, January 2019. doi: 10.1038/s41586-019-0873-4.
- [45] Eli Visbal, Zoltán Haiman, and Greg L. Bryan. Direct collapse black hole formation from synchronized pairs of atomic cooling haloes. *Monthly Notices of the Royal Astronomical Society*, 445(1):1056–1063, November 2014. doi: 10.1093/mnras/stu1794.
- [46] S. Peng Oh and Zoltán Haiman. Second-Generation Objects in the Universe: Radiative Cooling and Collapse of Halos with Virial Temperatures above 10^4 K. *The Astrophysical Journal*, 569(2):558–572, April 2002. doi: 10.1086/339393.
- [47] Volker Bromm and Abraham Loeb. Formation of the First Supermassive Black Holes. *The Astrophysical Journal*, 596(1):34–46, October 2003. doi: 10.1086/377529.

- [48] Bhaskar Agarwal and Sadegh Khochfar. Revised rate coefficients for H_2 and H^- destruction by realistic stellar spectra. *Monthly Notices of the Royal Astronomical Society*, 446(1):160–168, January 2015. doi: 10.1093/mnras/stu1973.
- [49] Bhaskar Agarwal, Fergus Cullen, Sadegh Khochfar, Daniel Ceverino, and Ralf S Klessen. Optimal neighbourhood to nurture giants: a fundamental link between star-forming galaxies and direct collapse black holes. *Monthly Notices of the Royal Astronomical Society*, 488(3):3268–3273, May 2019. ISSN 1365-2966. doi: 10.1093/mnras/stz1347. URL <http://dx.doi.org/10.1093/mnras/stz1347>.
- [50] Stephen Hawking. Black hole explosions? *Nature*, 248:1, jan 1974. doi: 10.1038/248030. URL <https://doi.org/10.1038/248030a0>.
- [51] Stephen Hawking. Gravitationally collapsed objects of very low mass. *Monthly Notices of the Royal Astronomical Society*, 152:75, January 1971. doi: 10.1093/mnras/152.1.75.
- [52] B. J. Carr and S. W. Hawking. Black holes in the early Universe. *Monthly Notices of the Royal Astronomical Society*, 168:399–416, August 1974. doi: 10.1093/mnras/168.2.399.
- [53] Boyuan Liu, Saiyang Zhang, and Volker Bromm. Effects of stellar-mass primordial black holes on first star formation. *Monthly Notices of the Royal Astronomical Society*, 514(2):2376–2396, August 2022. doi: 10.1093/mnras/stac1472.
- [54] Boyuan Liu and Volker Bromm. Impact of primordial black holes on the formation of the first stars and galaxies. *arXiv e-prints*, art. arXiv:2312.04085, December 2023. doi: 10.48550/arXiv.2312.04085.
- [55] Yifan Lu, Zachary S. C. Picker, and Alexander Kusenko. High-redshift supermassive black holes from tiny black hole explosions. *Physical Review D*, 109(12):123016, June 2024. doi: 10.1103/PhysRevD.109.123016.
- [56] Don N. Page. Particle emission rates from a black hole: Massless particles from an uncharged, nonrotating hole. *Physical Review D*, 13(2):198–206, January 1976. doi: 10.1103/PhysRevD.13.198.
- [57] Markus Mosbech and Zachary Picker. Effects of Hawking evaporation on PBH distributions. *SciPost Physics*, 13(4):100, October 2022. doi: 10.21468/SciPostPhys.13.4.100.
- [58] B. J. Carr. The primordial black hole mass spectrum. *Astrophysical Journal*, 201:1–19, October 1975. doi: 10.1086/153853.
- [59] Bernard Carr and Florian Kühnel. Primordial Black Holes as Dark Matter: Recent Developments. *Annual Review of Nuclear and Particle Science*, 70:355–394, October 2020. doi: 10.1146/annurev-nucl-050520-125911.
- [60] Albert Escrivà, Florian Kuhnel, and Yuichiro Tada. Primordial Black Holes. *arXiv e-prints*, art. arXiv:2211.05767, November 2022. doi: 10.48550/arXiv.2211.05767.
- [61] Christian T. Byrnes and Philippa S. Cole. Lecture notes on inflation and primordial black holes. *arXiv e-prints*, art. arXiv:2112.05716, December 2021. doi: 10.48550/arXiv.2112.05716.
- [62] Alexandre Arbey. Primordial black holes, a small review. *arXiv e-prints*, art. arXiv:2405.08624, May 2024. doi: 10.48550/arXiv.2405.08624.
- [63] Bernard Carr, Kazunori Kohri, Yuuiti Sendouda, and Jun’ichi Yokoyama. Constraints on primordial black holes. *Reports on Progress in Physics*, 84(11):116902, November 2021. doi: 10.1088/1361-6633/ac1e31.
- [64] Anne M. Green and Bradley J. Kavanagh. Primordial black holes as a dark matter candidate. *Journal of Physics G Nuclear Physics*, 48(4):043001, April 2021. doi: 10.1088/1361-6471/abc534.
- [65] Jérémy Auffinger. Primordial black hole constraints with Hawking radiation-A review. *Progress in Particle and Nuclear Physics*, 131:104040, July 2023. doi: 10.1016/j.pnpnp.2023.104040.
- [66] Zoltán Haiman, Tom Abel, and Martin J. Rees. The Radiative Feedback of the First Cosmological Objects. *The Astrophysical Journal*, 534(1):11–24, May 2000. doi: 10.1086/308723.
- [67] Kazuyuki Sugimura, Kazuyuki Omukai, and Akio K. Inoue. The critical radiation intensity for direct collapse black hole formation: dependence on the radiation spectral shape. *Monthly Notices of the Royal Astronomical Society*, 445(1):544–553, November 2014. doi: 10.1093/mnras/stu1778.
- [68] Bhaskar Agarwal, Britton Smith, Simon Glover, Priyamvada Natarajan, and Sadegh Khochfar. New constraints on direct collapse black hole formation in the early Universe. *Monthly Notices of the Royal Astronomical Society*, 459(4):4209–4217, July 2016. doi: 10.1093/mnras/stw929.
- [69] Bhaskar Agarwal, Jarrett L. Johnson, Erik Zackrisson, Ivo Labbe, Frank C. van den Bosch, Priyamvada Natarajan, and Sadegh Khochfar. Detecting direct collapse black holes: making the case for $\text{cr}7$. *Monthly Notices of the Royal Astronomical Society*, 460(4):4003–4010, May 2016. ISSN 1365-2966. doi: 10.1093/mnras/stw1173. URL <http://dx.doi.org/10.1093/mnras/stw1173>.

- [70] Bhaskar Agarwal, Fergus Cullen, Sadegh Khochfar, Ralf S. Klessen, Simon C. O. Glover, and Jarrett Johnson. Effects of binary stellar populations on direct collapse black hole formation. *Monthly Notices of the Royal Astronomical Society: Letters*, 468(1):L82–L86, February 2017. ISSN 1745-3933. doi: 10.1093/mnrasl/slx028. URL <http://dx.doi.org/10.1093/mnrasl/slx028>.
- [71] Muhammad A Latif and Sadegh Khochfar. UV regulated star formation in high-redshift galaxies. *Monthly Notices of the Royal Astronomical Society*, 490(2):2706–2716, October 2019. ISSN 1365-2966. doi: 10.1093/mnras/stz2812. URL <http://dx.doi.org/10.1093/mnras/stz2812>.
- [72] J. Wolcott-Green, Z. Haiman, and G. L. Bryan. Beyond J_{crit} : a critical curve for suppression of H_2 -cooling in protogalaxies. *Monthly Notices of the Royal Astronomical Society*, 469(3):3329–3336, August 2017. doi: 10.1093/mnras/stx167.
- [73] Andrea Incatasciato, Sadegh Khochfar, and Jose Oñorbe. Modelling the cosmological Lyman-Werner background radiation field in the early Universe. *Monthly Notices of the Royal Astronomical Society*, 522(1):330–349, June 2023. doi: 10.1093/mnras/stad1008.
- [74] Christopher C. Lovell, Ian Harrison, Yuichi Harikane, Sandro Tacchella, and Stephen M. Wilkins. Extreme value statistics of the halo and stellar mass distributions at high redshift: are JWST results in tension with Λ CDM? *Monthly Notices of the Royal Astronomical Society*, 518(2):2511–2520, January 2023. doi: 10.1093/mnras/stac3224.
- [75] Hannah O’Brennan, John A. Regan, and Chris Power. Halo mass functions at high redshift. *arXiv e-prints*, art. arXiv:2408.15194, August 2024. doi: 10.48550/arXiv.2408.15194.
- [76] Zoltán Haiman, Martin J. Rees, and Abraham Loeb. Destruction of Molecular Hydrogen during Cosmological Reionization. *The Astrophysical Journal*, 476(2):458–463, February 1997. doi: 10.1086/303647.
- [77] Eli Visbal, Zoltán Haiman, Bryan Terrazas, Greg L. Bryan, and Rennan Barkana. High-redshift star formation in a time-dependent Lyman-Werner background. *Monthly Notices of the Royal Astronomical Society*, 445(1):107–114, November 2014. doi: 10.1093/mnras/stu1710.
- [78] Anna T. P. Schauer, Boyuan Liu, and Volker Bromm. Constraining First Star Formation with 21 cm Cosmology. *The Astrophysical Journal Letters*, 877(1):L5, May 2019. doi: 10.3847/2041-8213/ab1e51.
- [79] Valeri P. Frolov and Igor D. Novikov. *Black hole physics : basic concepts and new developments*. Kluwer Academic, 1998.
- [80] Alexandre Arbey and Jérémy Auffinger. BlackHawk: a public code for calculating the Hawking evaporation spectra of any black hole distribution. *European Physical Journal C*, 79(8):693, August 2019. doi: 10.1140/epjc/s10052-019-7161-1.
- [81] Alexandre Arbey and Jérémy Auffinger. Physics beyond the standard model with BlackHawk v2.0. *European Physical Journal C*, 81(10):910, October 2021. doi: 10.1140/epjc/s10052-021-09702-8.
- [82] J. Traschen. An Introduction to Black Hole Evaporation. In Andrei A. Bytsenko and Floyd L. Williams, editors, *Mathematical Methods in Physics*, page 180, January 2000. doi: 10.48550/arXiv.gr-qc/0010055.
- [83] Sean M. Carroll. *Spacetime and Geometry: An Introduction to General Relativity*. Cambridge University Press, 2019. doi: 10.1017/9781108770385.
- [84] Greg L. Bryan and Michael L. Norman. Statistical Properties of X-Ray Clusters: Analytic and Numerical Comparisons. *The Astrophysical Journal*, 495(1):80–99, March 1998. doi: 10.1086/305262.
- [85] Zu-Cheng Chen and Alex Hall. Confronting primordial black holes with LIGO-Virgo-KAGRA and the Einstein Telescope. *arXiv e-prints*, art. arXiv:2402.03934, February 2024. doi: 10.48550/arXiv.2402.03934.